STAR Protocols

CellPress
OPEN ACCESS

Protocol

Microfluidic platform for spatially segregated experimental evolution studies with *E. coli*

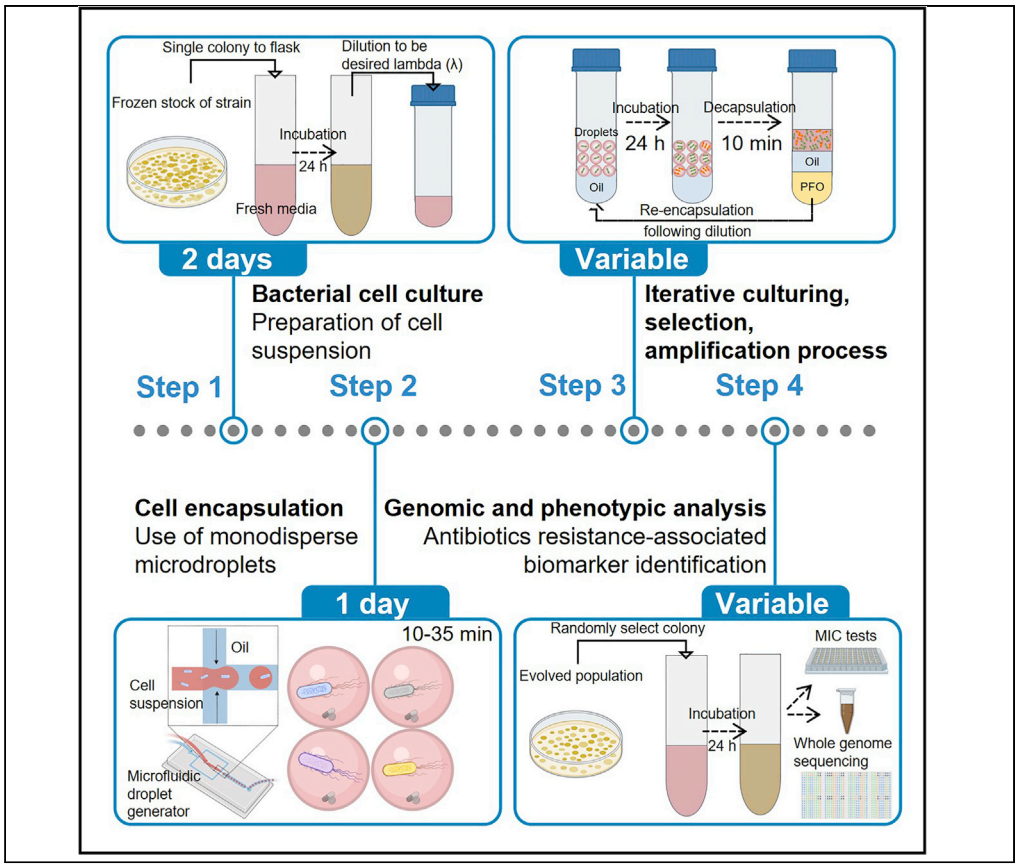

Microdroplet emulsions allow investigators to build controllable microenvironments for applications in experimental evolution and synthetic ecology. We designed a microfluidic platform that uses highly homogenous microdroplets to enable these experiments. We also present a step-by-step protocol for the rapid production of highly homogeneous microdroplets suitable for experimental evolution. We also describe protocols for the propagation and serial passage of microbial populations across a range of selection schemes and potential spatial structures.

Seokju Seo, Ramya Ganiga Prabhakar, Saoirse Disney-McKeethen, Xinhao Song, Yousif Shamoo

shamoo@rice.edu

Highlights

Microfluidics for the study of microbial evolution and biomarker discovery

Highly homogenous microdroplets as spatially segregated microenvironments

Platform to identify evolutionary trajectories leading to antimicrobial resistance

Seo et al., STAR Protocols 3, 101332
June 17, 2022
https://doi.org/10.1016/j.xpro.2022.101332

STAR Protocols

CellPress
OPEN ACCESS

Protocol

Microfluidic platform for spatially segregated experimental evolution studies with *E. coli*

Seokju Seo,[1,2] Ramya Ganiga Prabhakar,[1] Saoirse Disney-McKeethen,[1] Xinhao Song,[1] and Yousif Shamoo[1,3,*]

[1]Department of BioSciences, Rice University, Houston, TX 77005, USA

[2]Technical contact

[3]Lead contact

*Correspondence: shamoo@rice.edu
https://doi.org/10.1016/j.xpro.2022.101332

SUMMARY

Microdroplet emulsions allow investigators to build controllable microenvironments for applications in experimental evolution and synthetic ecology. We designed a microfluidic platform that uses highly homogenous microdroplets to enable these experiments. We also present a step-by-step protocol for the rapid production of highly homogeneous microdroplets suitable for experimental evolution. We also describe protocols for the propagation and serial passage of microbial populations across a range of selection schemes and potential spatial structures.

For complete details on the use and execution of this protocol, please refer to Seo et al. (2021).

BEFORE YOU BEGIN

The rise in drug-resistant bacterial infections threatens to undermine decades of biomedical progress (Kraker et al., 2016; Laupland et al., 2016). As the number of multi-drug and pan-resistant strains has increased it has become increasingly clear that understanding the evolutionary trajectories and biochemical mechanisms responsible for antimicrobial resistance play an important role in developing approaches in diagnostics, therapeutics, and drug discovery (Beabout et al., 2017). Recently, microfluidic techniques have been applied as a strategy to provide well-controlled user-designed environments for the study of cellular consortia, synthetic biology and now, experimental evolution (Alnahhas et al., 2019; Bachmann et al., 2013; Gupta et al., 2020; Hsu et al., 2019; Lawson et al., 2019; McDonald, 2019; van Tatenhove-Pel et al., 2021). Microdroplets-based approaches have the potential to provide a much broader range of experimental innovation that extends well beyond traditional batch serial transfer and bioreactor-based approaches (Seo et al., 2021). Importantly, microdroplet encapsulation of cells allows the investigator to impose spatial structure into their experiments. In well-mixed or batch experimental evolution studies, faster growing phenotypes are strongly favored. Serial propagation of microbial populations within microdroplets allows for the selection of efficient, yet slower-growing subpopulations (Bachmann et al., 2013). Thus, spatially segregated micro-environments can lead to unique evolutionary outcomes divorced from selection based on growth rate or clonal interference. In addition, microdroplet emulsions allow exquisite controllability of conditions, population sizes, the composition of cellular consortia and replication that allows the experimenter to investigate traditionally difficult to explore areas of the adaptive fitness landscape (Bachmann et al., 2013; Hsu et al., 2019). The production of microdroplets can be achieved by using either a vortex shaker (Reger et al., 2011) or stirred liquid/liquid systems (Lemenand et al., 2003) for generating polydisperse microdroplets and microdroplets-based microfluidics for monodisperse microdroplets. The water phase creates a thin neck near the junction of the

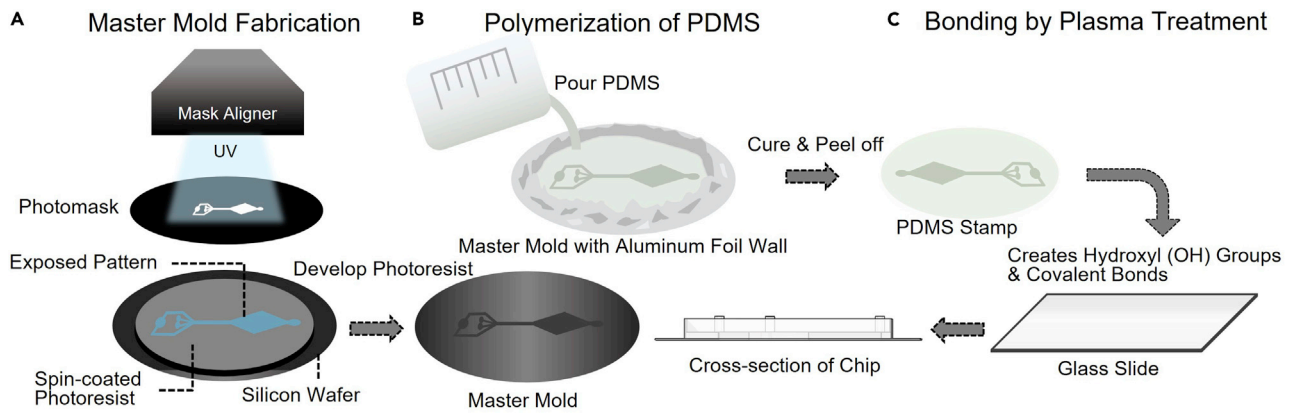

Figure 1. Schematic of photo and soft lithography

(A–C) Schematic of the photolithography process for (A) master mold fabrication and soft lithography process for microfluidic device fabrication, including (B) polymerization of the PDMS stamp using a fabricated master mold, and (C) bonding of the PDMS stamp to a glass microscope slide using plasma treatment.

microfluidic flow-focusing device, and the oil phase on both sides squeezes this neck. When a neck reaches the critical thickness, the neck is pinched-off, producing microdroplets (Lai et al., 2011; Mastiani et al., 2017). Microdroplets with diameter variation below 10% are considered monodisperse microdroplets (ten Klooster et al., 2019). The microfluidic chips developed for this study could readily produce highly homogeneous microdroplets with less than 1.5% variation. The microdroplet size and homogeneity determine the carrying capacity of the microdroplet that limits the total number of cells in each microdroplet. Since individual micro-compartment volumes differ in polydisperse microdroplets, it is difficult to exactly control initial number of cells within each microdroplet (λ) or their final cell number after incubation. On the other hand, the use of highly homogeneous microdroplets significantly improves controllability.

By including cycles or iterations of experimental evolution on cellular populations within emulsions, spatially segregated micro-environments can be varied both within and across cycles. Robust temporal, spatial, and selection environments can be used for long term experimental evolution and can include more than one species, interactions between host cells and pathogens as well as the investigation of biofilms (Gupta et al., 2020; Lawson et al., 2019). Although there is an enormous potential for microdroplets-based experimental evolution, adapting technology platforms is typically challenging and motivated us to develop protocols for microdroplets-based experimental evolution for use in the broader antimicrobial resistance, drug discovery, and evolution communities.

Microfluidic microdroplet generator fabrication

Timing: 2 days

Note: This section requires a patterned photomask of the optimized microchannel geometry design provided as supplemental data (Data S1, AutoCAD design of the microfluidic chip, related to step 6). A high-resolution transparency sheet (25,400 dpi) can be ordered from a photomasks printing company. The fabrication of master molds for microfluidic devices was performed in a cleanroom.

1. Photolithography (Figure 1A): If 4-inch silicon (Si) wafers are not clean, immerse them in acetone for 2–5 min followed by methanol for 1–2 min.
   a. Rinse them thoroughly with isopropanol.
   b. Remove the isopropanol by blowing pressurized nitrogen, and any leftover solvent is vaporized by placing wafers on a 100°C hot plate for 5 min.

2. Cover the spin coater bowl with aluminum foil and place a wafer into a spin coater.
3. Dispense approximately 3 mL of SU-8 2075 onto the center of the wafer.

⚠ CRITICAL: If air bubbles are trapped in deposited SU-8 2075 during this process, remove them using a 3 mL plastic transfer pipette. Otherwise, SU-8 structures could be damaged by tiny, trapped bubbles in the later steps.

4. After an exact centering of a wafer on the vacuum chuck, close the lid of a spin coater.
   a. Turn the vacuum on and spin at 500 rpm for 10 s with an acceleration of 100 rpm s^{-1}, ramp up to 3,000 rpm for 30 s with an acceleration of 300 rpm s^{-1} for the film thickness of 80 μm (see Permanent Epoxy Negative Photoresist data sheet available online https://kayakuam.com/wp-content/uploads/2019/09/SU-82000DataSheet2025thru2075Ver4.pdf).
5. Place a deposited wafer with a negative photoresist layer on a 65°C hot plate for 5 min followed by a 95°C hot plate for 10 min.
6. Attach the patterned photomask to a glass plate and place it on the top of a mask aligner.
   a. After alignment, expose the spin-coated photoresist on a silicon wafer to UV light with exposure energy 240 mJ cm^{-2} for 80 μm layer SU-8 structures.
   b. During UV exposure, photomask patterns from the transparency sheet are transferred to the Si wafer. Troubleshooting 1.
7. Place a UV exposed wafer on a 65°C hot plate for 5 min followed by a 95°C hot plate for 10 min. Troubleshooting 2.
8. After cooling the substrate at 20°C for 20–30 s, submerge the wafer in a glass dish filled with SU-8 developer for 10 min.

Note: The regions of the photoresist exposed to UV light become insoluble in a developing solution, whereas the unexposed areas are dissolved.

9. Wash the substrate with isopropanol for 10 s.

Note: If a white film is produced during isopropanol rinse, submerge the wafer again in a glass dish filled with SU-8 developer for 1–2 min.

10. Repeat the isopropanol rinse step, and any leftover solvent is removed by blowing pressurized nitrogen, finally fabricating a master mold.
11. Check the quality and thickness of the developed SU-8 structures using a stereomicroscope and a profilometer.

Pause point: A prepared master mold can be used immediately or kept for several months.

12. Soft lithography (Figure 1B): Weigh 30 g of polydimethylsiloxane (PDMS) resin and 3 g of its cross-linker at 10:1 weight ratio to a disposable mixing cup.
    a. Mix them thoroughly by stirring vigorously.
    b. Degas the mixture using a vacuum pump with a vacuum chamber.
13. Wrap a master mold with aluminum foil to build the wall for casting the PDMS mixture onto a master mold.
14. Pour the mixture onto a master mold and degas them again until no bubbles are being made.
15. After baking them at 80°C for at least 60 min in an oven, peel a PDMS stamp off from a master mold.

Note: Peel a PDMS stamp off at a high temperature immediately after removing it from the oven. After cooling down, the bonding strength between a PDMS stamp and a master mold is high, so that a master mold could be broken.

Pause point: A baked microfluidic stamp can be used immediately or kept for several months.

16. Punch the inlet and outlet holes (0.5 mm in diameter) using a biopsy punch at locations of a PDMS stamp.
17. After cutting along with the boundaries of individual PDMS devices using blades, remove debris on a PDMS device and a microscope slide using adhesive tape.

Optional: Microscope slides usually are supplied in pre-cleaned condition; however, if necessary, wash a microscope slide with isopropanol and ethanol. Blow-dry leftover solvent out with pressurized air.

18. Treat a PDMS device and a microscope slide with oxygen plasma using a radio frequency (RF) power within the range of 18–30 W for 2 min (Figure 1C). Troubleshooting 3 and 4.
    a. Face the channel side and a microscope slide surface in contact with PDMS upward.

Note: The hydroxyl (OH) group is formed onto a PDMS device's surfaces and a glass slide by oxygen plasma treatment. A PDMS device is covalently bonded to a glass slide by OH group reacted with the silanes.

⚠ CRITICAL: The power and duration of oxygen plasma treatment can be varied depending on the specific instruments used. Should be optimized following the manual. Poor bonding quality can lead to inconsistent microdroplets' size and eventually leakage of fluids during microfluidic operations.

Note: Inefficient bonding by mishandling plasma cleaner can lead to weak bonding between PDMS and microscope slide. Check plasma treatment power and duration.

Optimize these parameters (see Harrick Expanded Plasma Cleaner data sheet available online https://harrickplasma.com/plasma-cleaners/high-powered-expanded-plasma-cleaner/).

19. Attach the plasma-treated faces and gently tap the PDMS to remove the gap between them.
20. Bake it at 80°C for 1 day to enhance the bonding strength and restore the PDMS microchannels' hydrophilicity.

Microfluidic chip sterilization

Timing: 30–60 min

Note: Cell encapsulation requires transferring prepared growth media containing cells to the microfluidic chips and fluid handling consumables such as a syringe, syringe needle, tubing, etc. Special care needs to be taken to prevent microbial contamination when microfluidic chips are reused during experimental evolution.

21. Place PDMS microfluidic chips, syringes, syringe needles, and tubing on an autoclavable tray.
22. Autoclave at 121°C for 8 min wet cycle, 15 min dry cycle.
23. After connecting chips and syringe through the tubing, rinse with 70% ethanol followed by distilled water in a sterile environment such as a biosafety cabinet.
24. Before cell encapsulation, make empty microdroplets with fresh growth media and fluorinated oil containing 1.5 w/w% fluorinated surfactants to confirm that the generated microdroplets' size is consistent.

⚠ CRITICAL: Make sure to confirm changes in microdroplets size by chip damages during autoclave sterilization.

KEY RESOURCES TABLE

REAGENT or RESOURCE	SOURCE	IDENTIFIER
Bacterial and virus strains		
Escherichia coli strain BW25113	(Baba et al., 2006)	N/A
Other		
1H,1H,2H,2H-perfluoro-1-octanol	Sigma-Aldrich	Cat# 370533
Acetone	Sigma-Aldrich	Cat# 534064
Ethanol	Sigma-Aldrich	Cat# 459836
Fluorinated surfactant	Sphere Fluidics	Pico-Surf 1™
HFE-7500 oil	3M	Cat# 98-0212-2928-5
Isopropanol	Sigma-Aldrich	Cat# 278475
Negative photoresist	MicroChem	SU-8 2075
Polydimethylsiloxane (PDMS) and curing agent	Dow	SYLGARD 184, Cat. no. 1673921
Microscope slides	Thermo Fisher Scientific	Cat# 12-550-A3
Reusable biopsy punches (Diameter: 0.5 mm)	Electron Microscopy Sciences	Cat# 69038
Sterile syringes needles (23 gauge for 0.25-mm-diameter microtubing)	Terumo Neolus	Cat# NN2325R
PTFE microtubing (0.56 × 1.07 mm)	Fisher Scientific	Cat# W39241
Sterile syringes (3 mL)	Fisher Scientific	Cat# 14-823-435
Petri dishes (100-mm diameter × 15 mm)	BD Falcon	Cat# 351029
Twelve channel programmable syringe pump	New Era Pump Systems	NE-1200
Oven	Cole-Parmer	StableTemp digital mechanical convection oven
Scale	Denver Instrument	Cat# S-402
Centrifuge	Eppendorf	Cat# 5702
Inverted microscope for time-lapse imaging	Nikon	Eclipse Ti-2E
High-speed camera	Phantom	V7.2
Digital CMOS camera (2048 × 2048 with pixel array with 6.5 × 6.5-μm^2 pixel size)	Hamamatsu	ORCA Flash 4 LT
Pipettes	Eppendorf	P20, P200, and P1000
Sterile capillary tube	Thermo Fisher Scientific	Cat# 05-030-20
Vortex (LMS)	Dominique Dutscher	Cat# 079030
Disposable mixing cups	Dominique Dutscher	Cat# 045108
Aluminum foil	Thermo Fisher Scientific	Cat# 01-213-101
Vacuum desiccator	Sigma-Aldrich	Cat# D2672
Scalpel (No. 11)	Becton Dickinson	Cat# 371611
Oxygen plasma cleaner	Harrick Plasma	PDC-001
Mask aligner	EV Group	EVG 620
Spin coater	Laurell	WS-650MZ-23NPP

STEP-BY-STEP METHOD DETAILS

Bacterial cell culture

Timing: 2 days

1. Streak −80°C frozen stock containing strains of interest onto non-selective, nutrient-rich (e.g., Luria-Bertani) agar plates for isolation (Figure 3A).
   a. Incubate plates aerobically for 1 day at 37°C.
2. Prepare at least four tubes for one control group and three test populations (Recommend more than three biological replicates).
   a. Using a sterile loop or swab, select a single colony to add to each test tube containing 5 or 10 mL of sterile growth media (Figure 3B).
   b. Incubate in a shaker at 250 rpm at 37°C.
3. Measure OD_{600} values of cultures and convert them to the colony-forming unit (CFU) counts/mL using a standard curve as different microbial species can have different sizes.

	OD_{600}	CFU mL^{-1}
Escherichia coli	1.0	~2.6×10^8
Pseudomonas aeruginosa	1.0	~6.0×10^9
Streptomyces venezuelae	1.0	~7.3×10^8

4. Dilute with fresh growth media to achieve the desired lambda (λ), representing the average number of cells in each microdroplet (Figure 3C).

   Note: One or fewer cells are encapsulated in each microdroplet when the λ value is significantly lower than 1 thereby reducing clonal interference. At λ >1 encapsulated cells compete for resources and favor success of the faster growing variants. At λ< 1, more evolutionary trajectories can be maintained as slower growing phenotypes will not be readily eliminated by competition within the microdroplet. The experiment can thus be tuned for more or less clonal interference by altering λ and provides yet another controllable parameter for the investigator.

5. Prepare at least four populations of 2 mL growth media containing the desired number of cells to 50-mL conical-bottom tubes.

   ⚠ CRITICAL: Maintain the same λ value during experimental evolution to eliminate the effects of λ change on the evolutionary trajectories. We typically maintain the starting population of ~2.6×10^6 CFU mL^{-1} of *E. coli* in microdroplets of 247 ± 3.5 μm for ~20 λ. The average number of cells per microdroplet used was ~20. The choice of λ determines the extent of clonal interference within each microdroplet. Values of λ significantly less than 1 will dramatically decrease clonal interference and may allow the investigator to identify more evolutionary trajectories than higher values in which different variants within a microdroplet will compete against each other for resources based largely on growth rate. The number of cells in a microdroplet can be derived from the Poisson distribution, as $P(X = x) = \lambda^x e^{-\lambda}/x!$, where P is the probability of finding x cells per microdroplet and the parameter λ is the average number of cells per microdroplet which is calculated by multiplying the cell concentration by microdroplets volume.

Emulsions of microfluidic generated microdroplets can provide spatially segregated micro-environments in experimental evolution. Microorganisms of interest can be trapped within a microemulsion. One milliliter of emulsion contains millions of microdroplets (e.g., size 90 μm and volume ~380 pl) and thus, each milliliter can be thought of as having millions of individual bioreactors. We use an iterative cycle of encapsulation, adaptation/selection, and decapsulation followed by deep sequencing of the populations to identify genetic changes associated with antibiotics of interest. Figure 2 shows schematic diagrams of the geometry of microdroplets-based microfluidic and the protocol of serial propagation in the emulsion for experimental evolution. A flow-focusing geometry in a microfluidic chip consists of two microchannels (100 μm wide) for a dispersed phase and one microchannel (200 μm wide) for a continuous phase converging into the main microchannel (200 μm wide) for two-phase microdroplet flows. The height of all microchannels is 80 μm.

Founder cells are encapsulated in a water-in-oil emulsion system that includes the antibiotic. While the initially inoculated cells are reproduced within microdroplets, mutant cells that are resistant to an antibiotic are evolved. After incubation under appropriate conditions, the resistant cell multiplies to reach the carrying capacity of the microdroplet while the others may not grow at all or to a much lower density in the presence of antibiotics. In this highly simplified illustration, only 12 microdroplets are shown for simplicity on day 1. The microdroplets are broken for propagating the emulsion, and the cells are diluted in fresh media before inoculating into new emulsion microdroplets containing higher antibiotic concentrations. After dilution, if 5 resistant genotypes are encapsulated in new

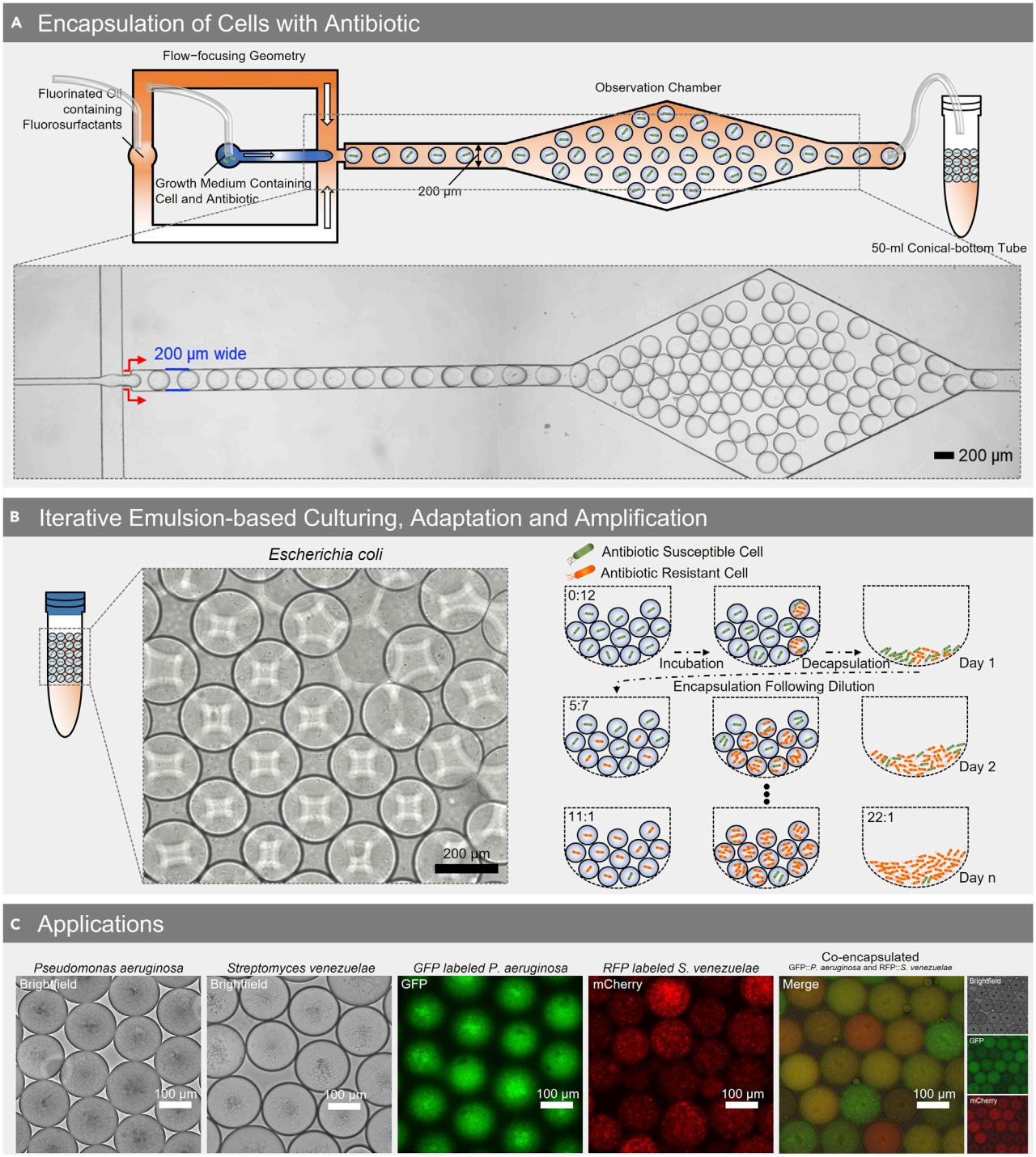

Figure 2. Microdroplets-based microfluidic platform for experimental evolution for identification of antimicrobial biomarkers or the production of synthetic ecologies for use in multi-species studies

(A) Encapsulation process: Antibiotic susceptible cell is compartmentalized in the desired size of microdroplets with an appropriate antibiotic concentration. Representative optical microscopy images of monodispersed microdroplets immediately after the junction and in the observation chamber are shown in the inset (Scale bar: 200 μm).

(B) Iterative culturing, selection, and amplification process: An optical micrograph of the compartmentalized model organism (*Escherichia coli*) after the incubation process is shown in the inset (Scale bar: 200 μm). For propagating the emulsion, the microdroplets are broken after incubation, and the cells are diluted in fresh media before inoculating into new emulsion microdroplets containing higher antibiotic concentrations. After dilution, if 5 resistant

Figure 2. *Continued*

variants are encapsulated in new microdroplets, then these can multiply once again. Through this repeated series of processes, the evolved resistant mutants increase in frequency with each iteration.

(C) Applications of microdroplets-based experimental evolution: Optical microscopy images of compartmentalized *Pseudomonas aeruginosa*, *Streptomyces venezuelae*, and fluorescence microscopy images of encapsulated green and red fluorescent proteins labeled *P. aeruginosa* and *S. venezuelae* and their co-encapsulation after the incubation process are shown in the inset (Scale bar: 100 μm).

emulsion microdroplets, then these can multiply once again. This cycle is then repeated, and the more resistant genotypes will increase in frequency with each iteration. At the end of the experiment, deep sequencing of the entire population and individual endpoint isolates will identify the genes associated with resistance to antibiotics. This section describes step-by-step instructions of cell encapsulation for one control and five biological replicates using prepared bacterial cell liquid cultures and microdroplet generators in the previous step as outlined in Figure 3.

Cell encapsulation

Timing: 10–35 min

6. Transfer each prepared population to a 3-mL sterile syringe in a biosafety cabinet.
7. Prepare six 3-mL sterile syringes containing 2 mL of fluorinated oil with 1.5% (wt/wt) fluorinated surfactants.
8. Affix one end of PTFE tubing to a sterile syringe needle and another one to the inlet of the PDMS microdroplets generator.
9. Load twelve 3-mL sterile syringes to a twelve-channel programmable syringe pump.
10. Start infusing with 100 μL min^{-1} of both flow rates for cell suspension and the continuous oil phase.

Note: Using parallelized six microfluidic chips, 247 ± 3.5 μm of the average diameter value with a standard deviation of microdroplets is generated for each population.

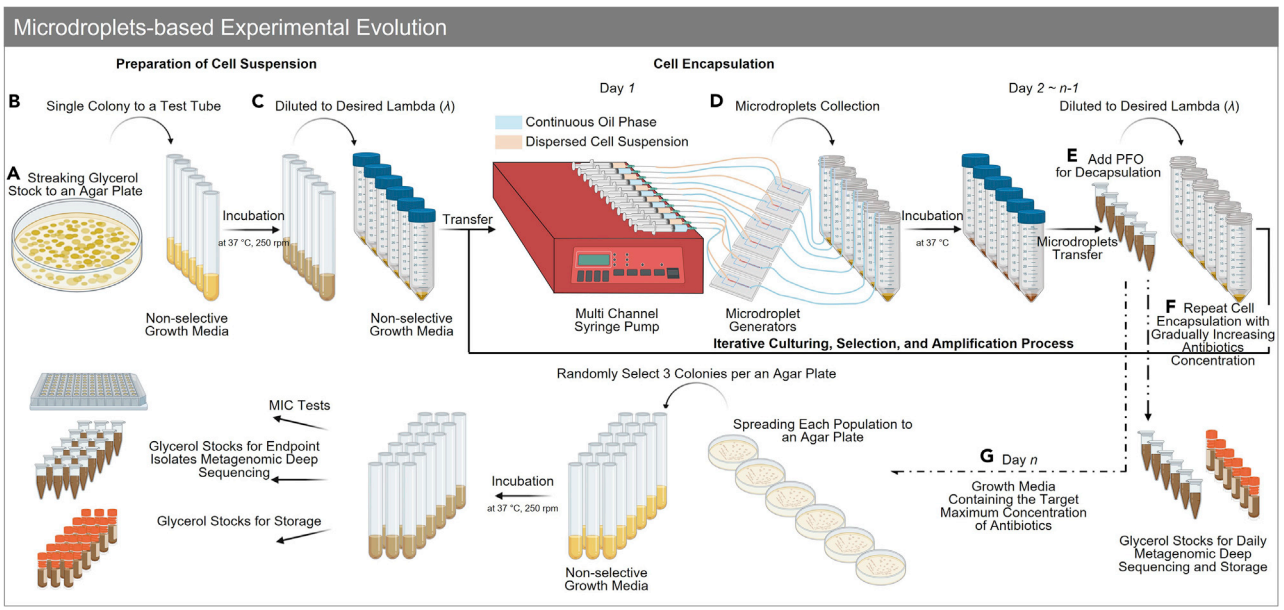

Figure 3. Schematic illustration of the workflow

Schematic overview of the workflow in the protocol for preparation of cell suspension, including (A) streaking glycerol stock to an agar plate; (B) selection of a single colony to add to each test tube; and (C) dilution with fresh growth media to achieve the desired lambda (λ); cell encapsulation, including (D) microdroplets collection; iterative culturing, selection, and amplification process, including (E) decapsulation; and (G) selection of evolved isolates in microdroplets-based experimental evolution

⚠ CRITICAL: Should confirm the size of microdroplets under the microscope before the operation in a biosafety cabinet. See Video S1. Recorded highly homogeneous microdroplets with a high-speed camera attached to an inverted microscope with a 10× objective lens, related to step 10. Troubleshooting 5. The ImageJ software, an open-source image processing program, can be used for analyses of microdroplet diameters. After collecting microscopy images of more than 50 microdroplets, their projected areas were used to calculate the diameters of microdroplets because they are an elongated shape when the diameter of microdroplets is longer than the wide or depth of the microchannel. Histograms of the microdroplet diameters are then made for evaluation. The average diameter values with standard deviations of microdroplets are accurately determined by fitting Gaussian or Lorentzian models to the histograms.

11. Collect ~2.0 mL of emulsions (1.0 mL of microdroplets) for each population to a 50-mL conical-bottom tube for 10 min (Figure 3D).

Note: The production rate of parallelized six microfluidic chips is 36 mL/h which is equivalent to 4.6×10^6 microdroplets/h (production rate of the individual chip is 6 mL/h, 7.6×10^5 microdroplets/h).

⚠ CRITICAL: In our optimal microdroplets-incubation method, we achieved a comparable bacterial growth rate within microdroplets compared to a flask, which was shaken for 24 h at 37°C using an orbital shaking incubator (calculation based on *E. coli*).

Iterative culturing, selection, and amplification process

Timing: Variable

We have optimized multiple parameters in this protocol, including the microdroplets incubation method, and selection strengths, which are the gradient of the daily controlled concentration of antibiotics to select evolved resistant mutants.

12. Incubate microdroplets containing *E. coli* at 37°C for 24 h.

13. Carefully transfer ~1.0 mL of microdroplets onto the oil surface from an old 50-mL conical-bottom tube to a new 1.5-mL Eppendorf tube for each population using a pipette.

⚠ CRITICAL: Used fluorinated oil containing 1.5 w/w% fluorinated surfactants can be recycled several times following filter sterilization through a 0.22 μm filter. Troubleshooting 5.

Optional: Use a sterile capillary tube to take microscopy images of microdroplets after incubation. Recommend using a capillary tube with a path length similar to microdroplets' diameter for a clear image as the morphology of microdroplets can be distorted by smaller path lengths.

14. After adding 250 μL of 1H,1H,2H,2H-perfluoro-1-octanol (PFO) to 1.0 mL of microdroplets, gently mix to break microdroplets by tapping a 1.5-mL Eppendorf tube with a finger for 30 s (Figure 3E). Troubleshooting 6.

Note: PFO can cause skin irritation and serious eye irritation. Use it only in a fume hood or a biosafety cabinet with appropriate laboratory clothing.

a. Leave the tubes in a biosafety cabinet for 5–10 min.

Note: When microdroplets are completely broken, the interface between oil and growth media containing *E. coli* becomes clear.

15. Pipette 100 μL of growth media containing *E. coli* for each population into each well of flat-bottom 96-well microplates. After measuring OD_{600} values of six populations using a microplate reader, calculate the volumes required for the desired λ in the next iteration.
16. Repeat 6–15 with gradually increasing antibiotic concentration until it reached four-fold of the antibiotic's clinical breakpoint (Figure 3F). Troubleshooting 7.

Note: Each population is diluted to the fresh media containing a higher concentration of antibiotics and the populations are not mixed at this step.

⚠ CRITICAL: When the density of *E. coli* is 1.71×10^8 CFU mL^{-1} after incubation, ~1.5% of dilution factor was used to get 2.6×10^6 CFU mL^{-1} of the starting population for the next iteration. The volume required for the serial propagation of a microbial population is variable depending on the growth kinetics of the organism within microdroplets and antibiotic concentration.

17. Mix 200 μL of collected cell suspension with 66.7 ul of 80% (vol/vol) sterile glycerol (20% (vol/vol) final concentration).
18. Prepare two glycerol stock solutions for each population, one for daily deep metagenomic sequencing from whole-community samples and another for storage.
19. Store the glycerol stock solutions at −80°C.
20. On the last day of experimental evolution when the concentration of antibiotics has reached the target maximum concentration, spread each population onto non-selective, nutrient-rich (e.g., Luria-Bertani) agar plates for the selection of evolved isolates following appropriate dilution (Figure 3G).
21. Randomly select a single colony to add to each test tube containing 5 or 10 mL of sterile growth media using a sterile loop or swab (Recommend more than three colonies per population).
22. Perform Minimum Inhibitory Concentration (MIC) test for endpoint isolates followed by preparing two glycerol stock solutions for each endpoint isolate and storing them at −80°C.

EXPECTED OUTCOMES

This protocol demonstrates a detailed procedure for a platform of experimental evolution by microdroplets. Upon completion of the experimental evolution described in this protocol, a microdroplet generator forming reliable monodispersed high-throughput microdroplets can be fabricated to collect desired volumes of water-in-oil emulsion containing resistant strains to get enough DNA yield from whole-community samples for deep metagenomic sequencing. We experimentally found the microdroplet incubation with a suitably large headspace volume method achieved comparable bacterial growth rates for *E. coli* within microdroplets compared to well-mixed flasks or tubes. To better understand the evolutionary dynamics in the propagation of a microbial population within microdroplets, we performed microdroplets-based experimental evolution with various selection strengths (Figure 4), which are the gradient of the daily controlled concentration of antibiotics to select evolved resistant mutants. One representative population of doxycycline-resistant *E. coli* evolved within microdroplets with the normal increase in selection strength is presented below in Table 1. Specifically, evolved *E. coli* from whole-community samples have changes consistent with increased expression of genes, such as *codA, cynR, acrR, tolB, marC, marR, setB, gabD, pstB, pstA,* and *rbsB* and were consistent with earlier biomarker discovery and clinical observations (Aly et al., 2012; Dunai et al., 2019; Seo et al., 2021; Toprak et al., 2012; Zhang et al., 2013). All doxycycline resistant *E. coli* in the population had adaptive mutations within *marR* while 22.2% carried an additional mutation in *acrR*. It is known that mutations in regulatory genes such as *marR* and *acrR*

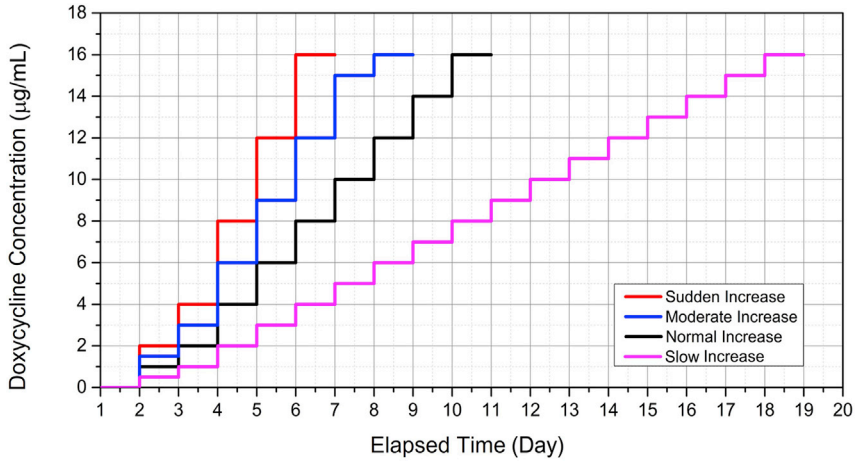

Figure 4. Different antibiotic selection gradients applied for microdroplets-based experimental evolution
The doxycycline concentration gradients used in each experiment and iteration were sub-inhibitory.

genes can lead to overexpression of the *acrA*/*acrB*/*tolC* multidrug efflux pump thereby contributing to antimicrobial resistance.

LIMITATIONS

Confining cells within a single microdroplet results in limited incubation up to 3–4 days due to the depletion of nutrients within microdroplets, physical limits in the number of cells a microdroplet can hold (carrying capacity) and microdroplet coalescence. Furthermore, since microdroplets cannot be shaken during the incubation without risking microdroplet coalescence achieving uniform and consistent aeration can be problematic. We found low bacterial growth in microdroplets resting at the bottom of the tube with insufficient aeration. To overcome this issue, the methods we tested for microfluidic strains culture in microdroplets include on-chip (Golberg et al., 2014; Pratt et al., 2019) and off-chip incubations in a capillary tube (Beneyton et al., 2016), 1.5 mL tubes (Chowdhury et al., 2019; Sjostrom et al., 2014) (Figure 5). In the first method of on-chip incubation, a chip capable of within the device incubation for microdroplets containing strains was fabricated (Figure 5A). This microfluidic device was composed of a flow-focusing geometry for generating monodispersed microdroplets and array geometry for incubation of microdroplets containing strains. This chip enables

Table 1. Mutations from whole-community samples for genetic changes of evolved doxycycline-resistant *E. coli* within microdroplets identified by whole-genome sequencing

Position	Mutation	Percentage	Annotation	Gene	Description	Ref
353,486	A→T	6.40%	intergenic (+321/+16)	*codA* → / ← *cynR*	Cytosine/isoguanine deaminase/transcriptional activator of cyn operon; autorepressor	
481,296	A→T	13.40%	Q27L (CAG→CTG)	*acrR* →	Transcriptional repressor	(Aly et al., 2012; Toprak et al., 2012)
481,787	G→A	8.80%	A191T (GCC→ACC)	*acrR* →	Transcriptional repressor	(Aly et al., 2012; Toprak et al., 2012)
773,303	T→C	5.10%	P36P (CCT→CCC)	*tolB* →	Periplasmic protein	
1,613,338	+TTAT CCCC	100%	intergenic (-173/-39)	*marC* ← / → *marR*	UPF0056 family inner membrane Protein /transcriptional repressor of multiple antibiotic resistance	(Aly et al., 2012; Dunai et al., 2019; Toprak et al., 2012)
2,257,640	C→T	5.60%	A100V (GCC→GTC)	*setB* →	lactose/glucose efflux system	
2,785,719	G→A	5.00%	R363H (CGC→CAC)	*gabD* →	Succinate-semialdehyde dehydrogenase I, NADP-dependent	
3,901,853	T→C	8.40%	intergenic (-127/+56)	*pstB* ← / ← *pstA*	Phosphate transporter subunit /phosphate Transporter subunit	
3,930,307	C→T	5.00%	R224C (CGC→TGC)	*rbsB* →	D-ribose transporter subunit	(Zhang et al., 2013)

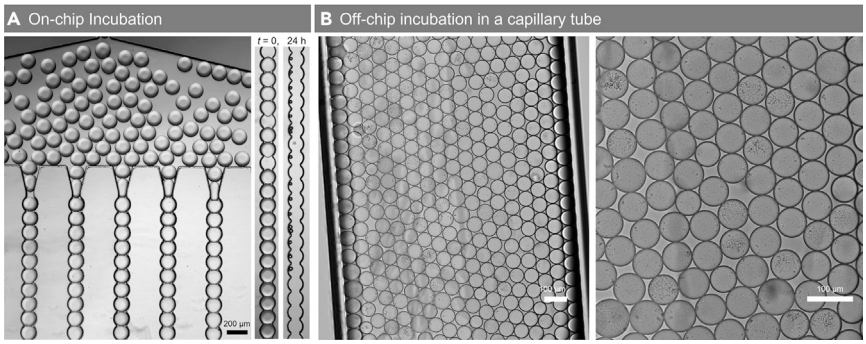

Figure 5. Types of incubation methods for microdroplets containing *E. coli*

(A) On-chip incubation with the microdroplets array device design (Scale bar: 200 μm).

(B) Off-chip incubations in a capillary tube (Scale bar: 100 μm).

the generation of 137.01 ± 1.39 μm microdroplets and incubation of 1.4×10^3 microdroplets. The second incubation method we tested was off-chip incubation using a glass capillary tube (Figure 5B). In both methods, microdroplet shrinkage due to the evaporation was observed during the incubation at 37°C. Although this microdroplet array technique and off-chip incubation in a capillary tube facilitate real-time observations of bacterial growth in microdroplets, the growth rate was significantly decreased by blocking the aeration to prevent microdroplet evaporation. To estimate an optimal ratio between microdroplets and headspace in 1.5 mL tubes allowing a surface area for comparable bacterial growth rate and the number of generations in microdroplets with a flask, the changes in the final OD_{600} of wild type *E. coli* at 24 *h* were examined in different ratios. The different emulsion volumes such as 200, 500, 1000, 1300, and 1,600 μL emulsions were collected in each 1.5 mL tube (maximum volume ~1.7 mL) while maintaining 0.01 of the initial OD_{600} of wild type *E. coli* in fresh media (Figure 6). Increasing the headspace from 100 to 1,500 μL, OD_{600} of wild type *E. coli* at 24 *h* increased growth significantly from 0.228 (4.43 doublings) to 0.67 (6.05 doublings) within the microdroplets. For comparison, the final OD_{600} of wild type *E. coli* in a flask was reached to be 0.82 (~6 doublings) when a flask was shaken for 24 *h* at 37°C using an orbital shaking incubator.

It is not accurate to assume that specific molecules cannot diffuse out of microdroplets. It has been shown that molecules such as N-acyl-homoserine lactones (AHLs) can diffuse readily. Confining metabolites within microdroplets < ~500 Daltons is limited since small and modestly lipophilic molecules may diffuse through currently commercially available fluorosurfactants, e.g., surfactants (Chowdhury et al., 2019; Gruner et al., 2016; Wagner et al., 2016).

The microdroplet features such as size and generation frequency can be altered by the design of the flow-focusing device as well as given flow rate conditions (Ngo et al., 2016). The microfluidic device channel for generating microdroplets less than a 74 μm diameter was adopted from Mazutis et al. (2013). Using 70 and 150 μL h^{-1} of the flow rates of cell suspension and 100 μL h^{-1} of the oil flow rate (Figures 7A and 7B), the average diameters with the standard deviations of microdroplets were 32.1 ± 0.5 and 35.1 ± 0.3 μm, respectively. Under these given flow rate conditions, the water phase neck's breakup points were near the junction. In the dripping regime, microdroplets are generally formed near the junction. As a result, the diameters of generated microdroplets were similar to the narrowest point (33.98 μm) of the junction channel. When the flow rates of cell suspension and oil were 20 μL h^{-1} (Figure 7C), we observed a dripping-jetting regimes transition. The water phase neck length was increased, and the breakup point moved from the junction to the main channel. In the jetting regime, since the dispersed neck's growth time is increased, microdroplets are generally formed at a point away from the junction. Because the downstream channel's width is gradually increased to 118.9 μm, the average diameter of microdroplets was increased to be 73.9 ± 1.0 μm. While maintaining the oil flow rate, when the water flow rate was increased to

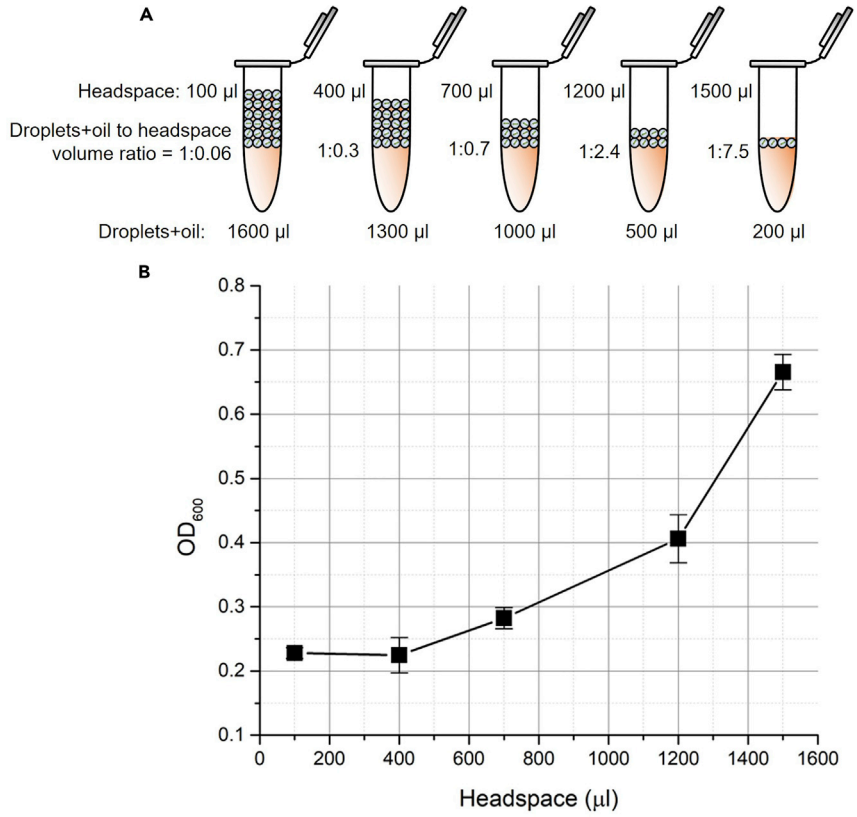

Figure 6. Effects of headspace on final OD600 of *E.coli*

(A) Off-chip incubations in 1.5 mL tubes with different volume ratios between 247 µm microdroplets+oil and headspace.

(B) The graph of changes in OD600 values of wild type *E. coli* within microdroplets incubated for 24 h as a function of headspace/emulsion ratio.

40 µL h^{-1}, we observed a jetting-stratified flow regime transition, i.e., a co-flowing water phase surrounded by oil streams (Figure 7D).

TROUBLESHOOTING

Problem 1

Small SU-8 structures are of poor quality.

Potential solution

Since this issue is related to over or under exposure of UV light, this can be solved by optimizing exposure time (Figure 8) (step 6 in before you begin).

Problem 2

Cracks in the SU-8 structures.

Potential solution

The sudden substrate temperature change may result in thermal stresses in the SU-8 film so that structures have cracks. When cooling down the substrate at 20°C in step 7 in before you begin, cool the wafer more slowly by placing it on a thermally insulating surface (Figure 9).

Problem 3

Weak bonding between PDMS and microscope slide.

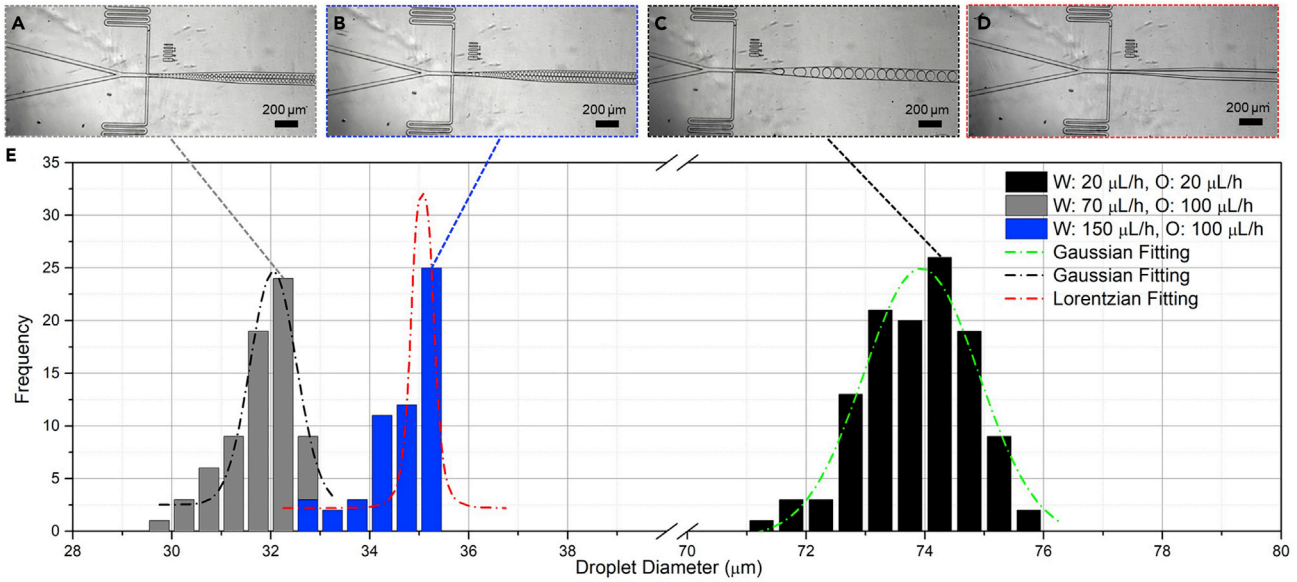

Figure 7. Microdroplet generator built for microdroplets-based experimental evolution

(A–D) Representative optical microscopy images of microdroplets as a function of different flow rates of (A) 70 and 100 μL h^{-1}, (B) 150 and 100 μL h^{-1}, (C) 20 and 20 μL h^{-1}, and (D) 40 and 20 μL h^{-1} for water (W) and oil (O) (Scale bar: 200 μm).

(E) Histograms of measured diameters of microdroplets.

Potential solution

Inefficient bonding by mishandling of plasma cleaner may lead to weak bonding between PDMS and slide, check plasma treatment power and duration to optimize these parameters in step 18 in before you begin.

Problem 4

Microfluidic device leaks.

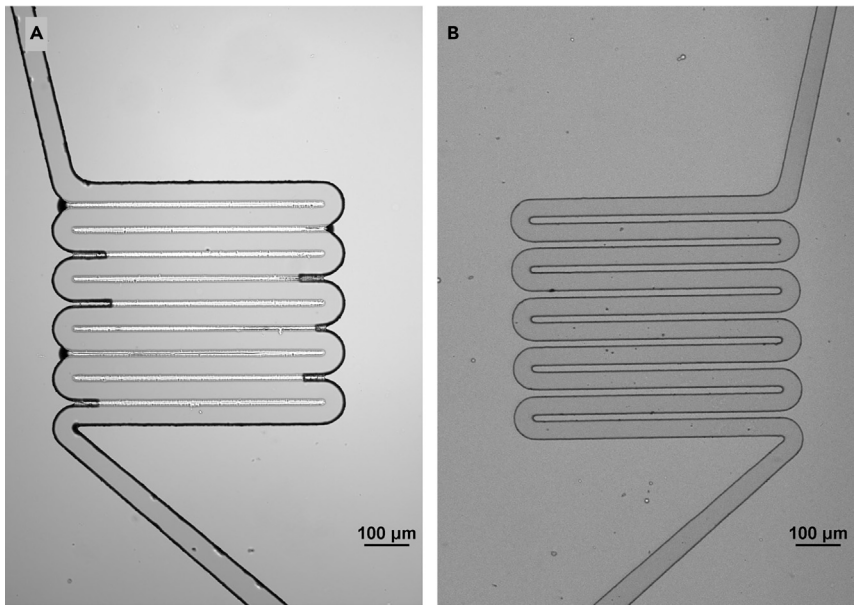

Figure 8. Failure in the fabrication of small SU-8 structures

(A and B) (A) Failed and (B) successful fabrications of a small serpentine microchannel (Scale bar: 100 μm).

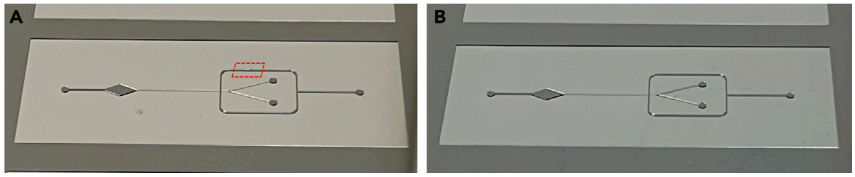

Figure 9. Some SU-8 structures have cracks due to thermal stress
(A and B) (A) Cracked and (B) even surfaces of SU-8 structures onto a silicon wafer.

Potential solution

If leaks from the inlets or outlet of chips, tearing surfaces of inlet PDMS may result in leaks. We recommend carefully inspecting the biopsy punch to make holes of inlets and an outlet and insert tubing. If leaks from between PDMS and microscope slide, weak bonding between PDMS and microscope slide may result in leaks. Check plasma treatment power and duration to optimize these parameters (step 18 in before you begin).

Problem 5

Microdroplets coalesce.

Potential solution

Since a low concentration of surfactants may lead to microdroplets coalescing, this can be solved by increasing surfactant concentration (Figure 10) (steps 10 and 13 in step-by-step method details).

Problem 6

Microdroplets do not break.

Potential solution

Poor mixing of perfluorooctanol with microdroplets may lead to this issue, we need to make sure that perfluorooctanol is correctly mixed with microdroplets (step 14 in step-by-step method details).

Problem 7

Cell density is too low after incubation.

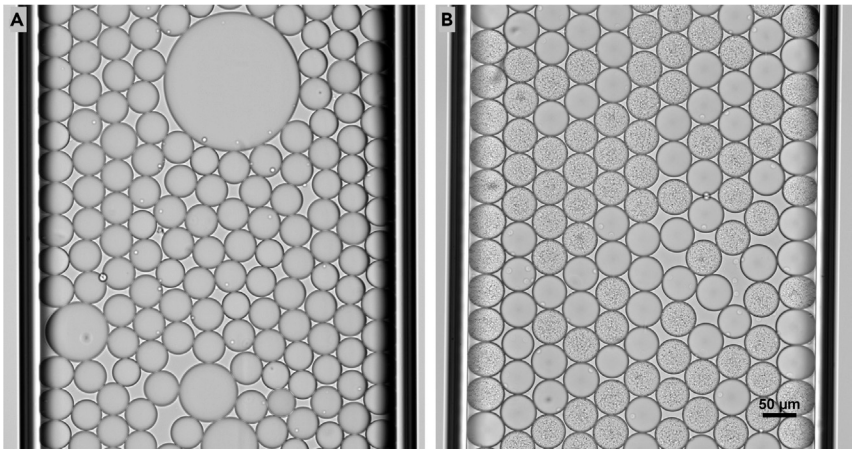

Figure 10. Microdroplets coalescence
(A and B) (A) Microdroplets coalescence immediately after their formation by the use of a low concentration of surfactants and (B) homogeneous monodisperse microdroplets with appropriate concentration of surfactants after 24 h incubation (Scale bar: 50 μm).

Potential solution

Since rapidly elevated antibiotic concentrations cause the organism to become extinct in step 16 in step-by-step method details, we recommend using a decreased gradient of the daily controlled concentration of antibiotics.

RESOURCE AVAILABILITY

Lead contact

Further information and requests for resources and reagents should be directed to and will be fulfilled by the lead contact, Yousif Shamoo (shamoo@rice.edu).

Materials availability

This study did not generate new unique reagents.

Data and code availability

This study did not generate datasets or code.

SUPPLEMENTAL INFORMATION

Supplemental information can be found online at https://doi.org/10.1016/j.xpro.2022.101332.

ACKNOWLEDGMENTS

This work is supported by funds from the Defense Threat Reduction Agency (HDTRA1-15-1-0069) and National Institute of Allergy and Infectious Diseases (R01A1080714) to Y.S. The content of the information in this paper does not necessarily reflect the position or the policy of the federal government, and no official endorsement should be inferred.

AUTHOR CONTRIBUTIONS

Y.S designed the study. S.S. and S.D.M. conducted experiments. S.S., S.D.M., R.G.P., X.S., and Y.S. analyzed data. All authors wrote the manuscript and read, edited, and approved the final manuscript.

DECLARATION OF INTERESTS

The authors declare no competing interests.

REFERENCES

Alnahhas, R.N., Winkle, J.J., Hirning, A.J., Karamched, B., Ott, W., Josić, K., and Bennett, M.R. (2019). Spatiotemporal dynamics of synthetic microbial consortia in microfluidic devices. ACS Synth. Biol. *8*, 2051–2058. https://doi.org/10.1021/acssynbio.9b00146.

Aly, S.A., Debavalya, N., Suh, S.-J., Oryazabal, O.A., and Boothe, D.M. (2012). Molecular mechanisms of antimicrobial resistance in fecal *Escherichia coli* of healthy dogs after enrofloxacin or amoxicillin administration. Can. J. Microbiol. *58*, 1288–1294. https://doi.org/10.1139/w2012-105.

Baba, T., Ara, T., Hasegawa, M., Takai, Y., Okumura, Y., Baba, M., Datsenko, K.A., Tomita, M., Wanner, B.L., and Mori, H. (2006). Construction of Escherichia coli K-12 in-frame, single-gene knockout mutants: the Keio collection. Mol. Syst. Biol. *2*, 2006.0008. https://doi.org/10.1038/msb4100050.

Bachmann, H., Fischlechner, M., Rabbers, I., Barfa, N., Branco dos Santos, F., Molenaar, D., and Teusink, B. (2013). Availability of public goods shapes the evolution of competing metabolic strategies. Proc. Natl. Acad. Sci. U S A *110*, 14302–14307. https://doi.org/10.1073/pnas.1308523110.

Beabout, K., McCurry, M.D., Mehta, H., Shah, A.A., Pulukuri, K.K., Rigol, S., Wang, Y., Nicolaou, K.C., and Shamoo, Y. (2017). Experimental evolution of diverse strains as a method for the determination of biochemical mechanisms of action for novel pyrrolizidinone antibiotics. ACS Infect. Dis. *3*, 854–865. https://doi.org/10.1021/acsinfecdis.7b00135.

Beneyton, T., Wijaya, I.P.M., Postros, P., Najah, M., Leblond, P., Couvent, A., Mayot, E., Griffiths, A.D., and Drevelle, A. (2016). High-throughput screening of filamentous fungi using nanoliter-range droplet-based microfluidics. Sci. Rep. *6*, 27223. https://doi.org/10.1038/srep27223.

Chowdhury, M.S., Zheng, W., Kumari, S., Heyman, J., Zhang, X., Dey, P., Weitz, D.A., and Haag, R. (2019). Dendronized fluorosurfactant for highly stable water-in-fluorinated oil emulsions with minimal inter-droplet transfer of small molecules. Nat. Commun. *10*, 4546. https://doi.org/10.1038/s41467-019-12462-5.

Dunai, A., Spohn, R., Farkas, Z., Lázár, V., Györkei, Á., Apjok, G., Boross, G., Szappanos, B., Grézal, G., Faragó, A., et al. (2019). Rapid decline of bacterial drug-resistance in an antibiotic-free environment through phenotypic reversion. eLife *8*. https://doi.org/10.7554/eLife.47088.

Golberg, A., Linshiz, G., Kravets, I., Stawski, N., Hillson, N.J., Yarmush, M.L., Marks, R.S., and Konry, T. (2014). Cloud-enabled microscopy and droplet microfluidic platform for specific detection of Escherichia coli in water. PLoS One *9*, e86341. https://doi.org/10.1371/journal.pone.0086341.

Gruner, P., Riechers, B., Semin, B., Lim, J., Johnston, A., Short, K., and Baret, J.-C. (2016). Controlling molecular transport in minimal emulsions. Nat. Commun. *7*, 10392. https://doi.org/10.1038/ncomms10392.

Gupta, S., Ross, T.D., Gomez, M.M., Grant, J.L., Romero, P.A., and Venturelli, O.S. (2020). Investigating the dynamics of microbial consortia in spatially structured environments. Nat. Commun. *11*, 2418. https://doi.org/10.1038/s41467-020-16200-0.

Hsu, R.H., Clark, R.L., Tan, J.W., Ahn, J.C., Gupta, S., Romero, P.A., and Venturelli, O.S. (2019). Microbial interaction network inference in microfluidic droplets. Cell Syst. *9*, 229–242.e4. https://doi.org/10.1016/j.cels.2019.06.008.

Kraker, M.E.A.de., Stewardson, A.J., and Harbarth, S. (2016). Will 10 million people die a year due to antimicrobial resistance by 2050? PLoS Med. *13*, e1002184. https://doi.org/10.1371/journal.pmed.1002184.

Lai, D., Frampton, J.P., Sriram, H., and Takayama, S. (2011). Rounded multi-level microchannels with orifices made in one exposure enable aqueous two-phase system droplet microfluidics. Lab Chip *11*, 3551. https://doi.org/10.1039/c1lc20560a.

Laupland, K.B., Ruppé, E., and Harbarth, S. (2016). In 2035, will all bacteria be multidrug resistant? We are not sure. Intensive Care Med. *42*, 2021–2023. https://doi.org/10.1007/s00134-016-4343-2.

Lawson, C.E., Harcombe, W.R., Hatzenpichler, R., Lindemann, S.R., Löffler, F.E., O'Malley, M.A., García Martín, H., Pfleger, B.F., Raskin, L., Venturelli, O.S., et al. (2019). Common principles and best practices for engineering microbiomes. Nat. Rev. Microbiol. *17*, 725–741. https://doi.org/10.1038/s41579-019-0255-9.

Lemenand, T., Della Valle, D., Zellouf, Y., and Peerhossaini, H. (2003). Droplets formation in turbulent mixing of two immiscible fluids in a new type of static mixer. Int. J. Multiphase Flow *29*, 813–840. https://doi.org/10.1016/S0301-9322(03)00032-6.

Mastiani, M., Seo, S., Jimenez, S.M., Petrozzi, N., and Kim, M.M. (2017). Flow regime mapping of aqueous two-phase system droplets in flow-focusing geometries. Colloids Surf. A Physicochem. Eng. Aspects *531*, 111–120. https://doi.org/10.1016/j.colsurfa.2017.07.083.

Mazutis, L., Gilbert, J., Ung, W.L., Weitz, D.A., Griffiths, A.D., and Heyman, J.A. (2013). Single-cell analysis and sorting using droplet-based microfluidics. Nat. Protoc. *8*, 870–891. https://doi.org/10.1038/nprot.2013.046.

McDonald, M.J. (2019). Microbial experimental evolution – a proving ground for evolutionary theory and a tool for discovery. EMBO Rep. *20*. https://doi.org/10.15252/embr.201846992.

Ngo, I.-L., Woo Joo, S., and Byon, C. (2016). Effects of junction angle and viscosity ratio on droplet formation in microfluidic cross-junction. J. Fluids Eng. *138*, 051202. https://doi.org/10.1115/1.4031881.

Pratt, S.L., Zath, G.K., Akiyama, T., Williamson, K.S., Franklin, M.J., and Chang, C.B. (2019). DropSOAC: stabilizing microfluidic drops for time-lapse quantification of single-cell bacterial physiology. Front. Microbiol. *10*. https://doi.org/10.3389/fmicb.2019.02112.

Reger, M., Sekine, T., Okamoto, T., and Hoffmann, H. (2011). Unique emulsions based on biotechnically produced hydrophobins. Soft Matter *7*, 8248–8257. https://doi.org/10.1039/C1SM06155K.

Seo, S., Disney-McKeethen, S., Prabhakar, R.G., Song, X., Mehta, H.H., and Shamoo, Y. (2021). Identification of evolutionary trajectories associated with antimicrobial resistance using microfluidics. ACS Infect. Dis. https://doi.org/10.1021/acsinfecdis.1c00564.

Sjostrom, S.L., Bai, Y., Huang, M., Liu, Z., Nielsen, J., Joensson, H.N., and Andersson Svahn, H. (2014). High-throughput screening for industrial enzyme production hosts by droplet microfluidics. Lab Chip *14*, 806–813. https://doi.org/10.1039/c3lc51202a.

ten Klooster, S., Sahin, S., and Schroën, K. (2019). Monodisperse droplet formation by spontaneous and interaction based mechanisms in partitioned EDGE microfluidic device. Sci. Rep. *9*, 7820. https://doi.org/10.1038/s41598-019-44239-7.

Toprak, E., Veres, A., Michel, J.-B., Chait, R., Hartl, D.L., and Kishony, R. (2012). Evolutionary paths to antibiotic resistance under dynamically sustained drug selection. Nat. Genet. *44*, 101–105. https://doi.org/10.1038/ng.1034.

van Tatenhove-Pel, R.J., Zwering, E., Boreel, D.F., Falk, M., van Heerden, J.H., Kes, M.B.M.J., Kranenburg, C.I., Botman, D., Teusink, B., and Bachmann, H. (2021). Serial propagation in water-in-oil emulsions selects for Saccharomyces cerevisiae strains with a reduced cell size or an increased biomass yield on glucose. Metab. Eng. *64*, 1–14. https://doi.org/10.1016/j.ymben.2020.12.005.

Wagner, O., Thiele, J., Weinhart, M., Mazutis, L., Weitz, D.A., Huck, W.T.S., and Haag, R. (2016). Biocompatible fluorinated polyglycerols for droplet microfluidics as an alternative to PEG-based copolymer surfactants. Lab Chip *16*, 65–69. https://doi.org/10.1039/C5LC00823A.

Zhang, P.-Y., Xu, P.-P., Xia, Z.-J., Wang, J., Xiong, J., and Li, Y.-Z. (2013). Combined treatment with the antibiotics kanamycin and streptomycin promotes the conjugation of *Escherichia coli*. FEMS Microbiol. Lett. *348*, 149–156. https://doi.org/10.1111/1574-6968.12282.